

Degradation Processes in High Power Multi-Mode InGaAs Strained Quantum Well Lasers

Yongkun Sin*, Nathan Presser, Brendan Foran, and Steven C. Moss
Electronics and Photonics Laboratory
The Aerospace Corporation
El Segundo, CA 90245-4691

ABSTRACT

Recently, broad-area InGaAs-AlGaAs strained quantum well (QW) lasers have attracted much attention because of their unparalleled high optical output power characteristics that narrow stripe lasers or tapered lasers can not achieve. However, broad-area lasers suffer from poor beam quality and their high reliability operation has not been proven for communications applications. This paper concerns reliability and degradation aspects of broad-area lasers. Good facet passivation techniques along with optimized structural designs have led to successful demonstration of reliable 980nm single-mode lasers, and the dominant failure mode of both single-mode and broad-area lasers is catastrophic optical mirror damage (COMD), which limits maximum output powers and also determines operating output powers. Although broad-area lasers have shown characteristics unseen from single-mode lasers including filamentation, their effects on long-term reliability and degradation processes have not been fully investigated. Filamentation can lead to instantaneous increase in optical power density and thus temperature rise at localized areas through spatial-hole burning and thermal lensing which significantly reduces filament sizes under high power operation, enhancing the COMD process. We investigated degradation processes in commercial MOCVD-grown broad-area InGaAs-AlGaAs strained QW lasers at ~975nm with and without passivation layers by performing accelerated lifetests of these devices followed by failure mode analyses with various micro-analytical techniques. Since instantaneous fluctuations of filaments can lead to faster wear-out of passivation layer thus leading to facet degradation, both passivated and unpassivated broad-area lasers were studied that yielded catastrophic failures at the front facet and also in the bulk. Electron beam induced current technique was employed to study dark line defects (DLDs) generated in degraded lasers stressed under different test conditions and focused ion beam was employed to prepare TEM samples from the DLD areas for HR-TEM analysis. We report our in-depth failure mode analysis results.

Keywords: High power lasers, strained quantum well lasers, broad area lasers, reliability, failure modes

1. INTRODUCTION

Broad-area InGaAs-AlGaAs strained quantum well (QW) single emitters in the lasing wavelength of 915-980nm have become indispensable as pump lasers for fiber lasers and amplifiers. High performance characteristics and high reliability are required from these pump lasers in communications applications including terrestrial and submarine optical networks as well as potential space satellite systems. Continuous efforts in chip design, crystal growth, fabrication, and packaging have led to an optical output power of over 20W and a power conversion efficiency of over 70% under CW operation [1-5]. However, major applications of these parts are still in industrial use that does not require stringent reliability from these parts. Thus, reliability of broad-area InGaAs-AlGaAs strained QW lasers still remains a major concern in high reliability applications including potential satellite systems. Before the broad-area lasers are fully deployed in long-term high reliability applications, a number of issues need to be carefully addressed including the effect of filamentation [6-12] on degradation processes and understanding of degradation mechanisms leading to facet failure and bulk failure. Catastrophic optical mirror damage has been extensively investigated, but almost no reports on bulk damage from broad-area lasers have been presented. Several groups investigated failure modes in broad-area lasers in recent years [13-15]. Our group also recently reported failure mode investigation of broad-area lasers using electron beam induced current (EBIC) and high-resolution transmission electron microscope (HR-TEM) techniques [16, 17].

*yongkun.sin@aero.org; phone (310) 336-1734; fax (310) 336-5846

In the present study, we report our investigation on degradation processes in broad-area InGaAs strained QW single emitters using various analytical techniques including EBIC, focused ion beam (FIB), and HR-TEM.

2. DEVICES, LIFETESTS, and FMA

Devices Laser diodes under study were commercial multi-mode broad-area lasers with a cavity length of ~ 2.5 mm and active region width of $\sim 100\mu\text{m}$. All the laser diodes studied consisted of strained InGaAs-AlGaAs single QW graded index (GRIN) separate confinement heterostructures (SCH) grown by metal-organic chemical vapor deposition (MOCVD). We investigated both unpassivated and passivated laser diode chips, which were mounted on C-mounts with indium solder. Among a total of 40 devices studied including 25 unpassivated and 15 passivated devices, ~ 30 EBIC samples were prepared using laser diodes that failed during lifetests or those forced to fail by electrical overstress to intentionally introduce catastrophic optical mirror damage (COMD). Table 1 summarizes 7 samples.

Table 1. Summary of samples used in this study for EBIC imaging.

Sample	Passivation Layer	Test Method	Failure Mode	Drop in Optical Power (%)
A	No	Lifetest (5A/65°C)	Facet Failure	~ 50
B	No	Electrical overstress	Facet Failure	~ 85
C	No	Electrical overstress	Facet Failure	~ 95
D	No	Lifetest (5A/65°C)	Facet Failure	~ 55
E	Yes	Lifetest (5A/65°C)	Bulk Failure	~ 60
F	Yes	Lifetest (6A/65°C)	Bulk Failure	~ 100
G	Yes	Lifetest (5A/65°C)	Bulk Failure	~ 25

Lifetests A commercial laser reliability tester was employed to introduce failures to all the laser diodes studied. Test conditions used for unpassivated devices were stress currents of 4 and 5A at a base-plate temperature of 65°C, whereas test conditions for passivated devices were stress currents of 4, 5, 6, and 7A at the same base-plate temperature of 65°C. Typical test duration of each accelerated lifetest was 720 hours. A series of accelerated lifetests were performed under automatic current control (ACC) mode and one of lifetest results is shown in Figure 1.

FMA Various destructive physical analysis instruments were employed to study failure modes of degraded broad-area lasers. EBIC, a technique that enables observation of localized defects in p-n junctions [18], has been employed to investigate failure modes in various types of semiconductor devices including semiconductor lasers [19, 20]. The objective of our EBIC study was to identify locations of dark line defects in degraded multi-mode lasers to make it possible to perform further failure mode analysis with FIB and HR-TEM. Our EBIC set-up, which was previously described [17], employed the focused ion beam system, Strata 235 from FEI as a SEM chamber. After dark line defects were identified from degraded laser diode chips using the EBIC technique, two dual-beam focused ion beam systems (FEI Strata Model 235 and 400) were used to prepare both cross sectional and plan view TEM samples for defect analysis using the 300keV HR-TEM (JEOL Model 3100F).

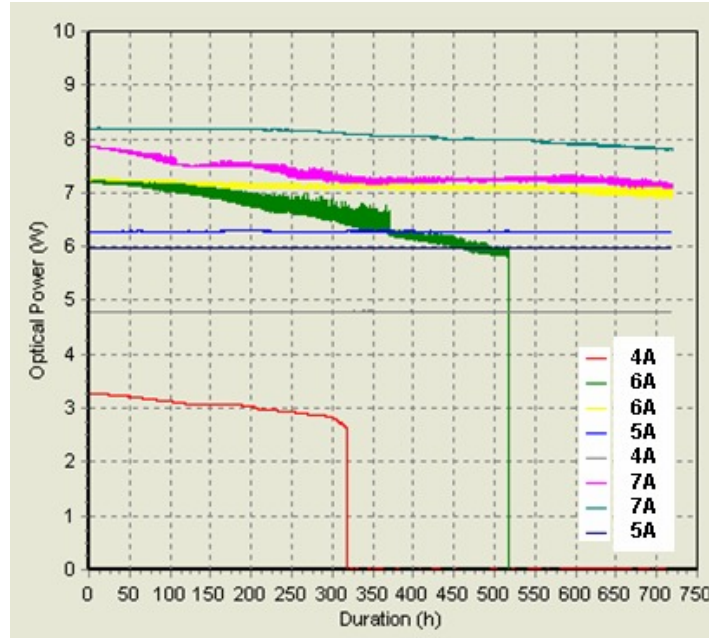


Figure 1. Accelerated lifetest result.

3. FACET DEGRADATION

Facet degradation occurs when optical power density at the front facet reaches a COMD threshold for single-mode lasers. When single-mode lasers undergo the COMD process at the facet, the significant increase in temperature in the vicinity of the center of optical beam leads to melting of materials followed by re-crystallization that creates a high density of dislocations. The COMD process in single-mode InGaAs-AlGaAs strained QW lasers has been extensively investigated for over a decade and the significant increase in facet temperature is attributed to carriers from the surface currents as well as from absorption of lasing photons that eventually leads to facet melting at localized area. A blister is typically created on the front facet when melting occurs. The same process is expected to occur in broad-area InGaAs-AlGaAs strained QW lasers simply because they are constructed using the same materials systems as for the single-mode lasers.

However, COMD thresholds are significantly lower in broad-area lasers than in single-mode lasers. Unlike single-mode lasers that show a Gaussian distribution of optical beam in lateral direction, broad-area lasers show multiples of filaments. Filamentation is a result of nonlinear interaction between carriers and optical fields that occurs on the psec time scale. Filament size (W) can be approximated using the ABCD matrix method and is given by (1).

$$W \cong \frac{\lambda}{\pi \sqrt{2n_c \cdot \Delta n}} \quad (1)$$

where λ is the lasing wavelength, n_c is the nominal refractive index, and Δn is the change in refractive index. Δn is due to various contributions including the built-in refractive index step, thermal effects, carrier induced change as well as optical nonlinear effects. The nonlinear refractive index or the Kerr coefficient depends on carrier density and temperature. As equation (1) indicates, the filament size can be significantly influenced by the change in refractive index. For example, for broad-area lasers with λ of 940nm and n_c of 3.5, the filament size reduces from 9.92 μ m to 5.06 μ m when Δn changes from 10^{-4} to 5×10^{-4} . This reduction in filament size leads to an increase in optical power density per filament from 4.7 to 9.3 MW/cm² assuming a vertical mode size of 1.5 μ m and uniform distribution of 7W optical power among 10 filaments. This change in optical power density per filament significantly impacts reliability of broad-area lasers and supports the model that filamentation plays a critical role in reducing the COMD threshold in broad-area lasers. In addition, the filament intensity can grow as the beam propagates along the laser cavity as a result of self-focusing of light. Also, filamentation might be responsible for

anomalies that we observed from our previous lifetests where some devices under lower stress conditions failed sooner than those under higher stress, making estimation of reliability model parameters meaningless [16].



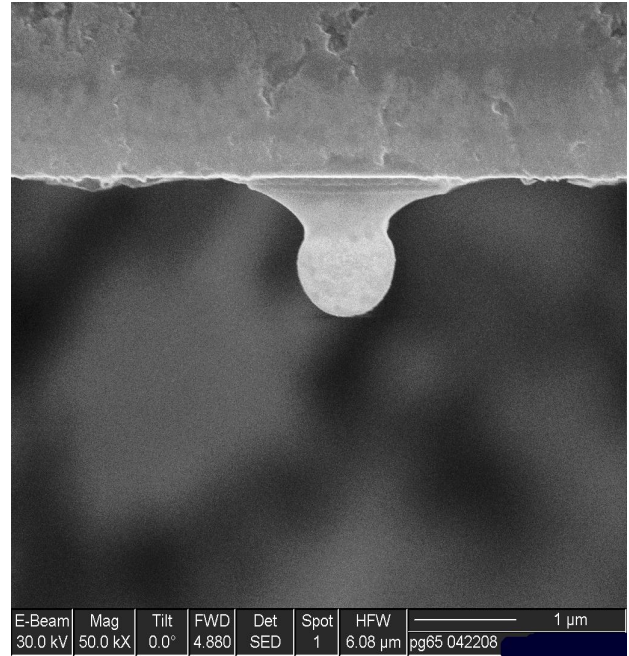
Figure 2. EBIC images from Sample A. EBIC images showing the whole chip (a) and front facet area (b) of Sample A.

When devices failed during accelerated lifetests, the failed devices were not under continuous stress until their removal from the tester. An automatic shut-off feature was introduced to avoid unwanted excessive overheating of the samples until their removal as part of our efforts to study the physics of failure in broad-area lasers at different stages of degradation. After the failures were removed from the tester, EBIC samples were prepared to identify failure modes by observing dark line defects. Table 1 shows four samples that showed facet failure.

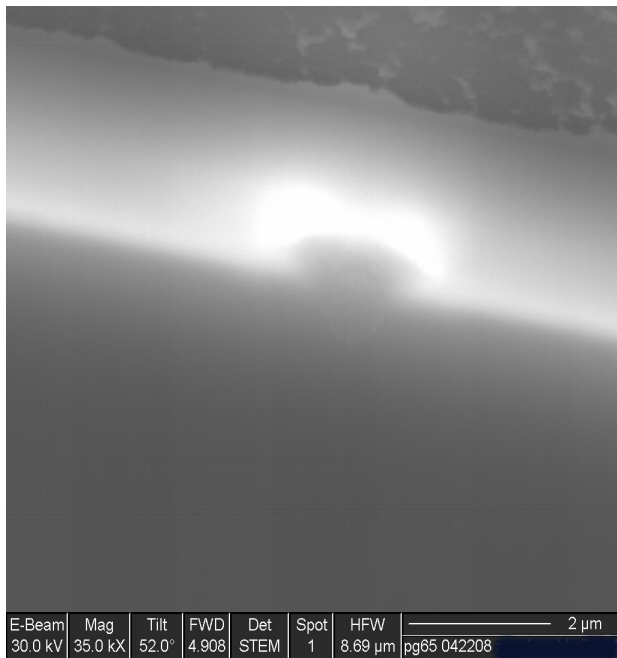
Figure 2 shows EBIC images showing the entire chip (a) and front facet area (b) of Sample A, which was lifetested at 5A and a baseplate temperature of 65°C. This sample showed an ~50% drop in optical power. DLDs of Sample A originated from the front facet, indicating that this sample failed by COMD. Figure 3 (a) and (c) shows EBIC images from Sample B and Figure 3 (d) shows an EBIC image from Sample C. Both samples were electrically overstressed at 7A and the baseplate temperature of 25°C to intentionally increase optical power density at the front facet above a threshold for COMD. Both samples showed significant amounts of drop in optical output power. Sample B showed a ~85% drop, whereas Sample C showed a ~95% drop. DLDs of Sample B and Sample C (DLDs of Sample C not shown here) impacted the front facet, consistent with the observation of COMD. Significant heating at the front facet created a blister for both samples. Figure 3 (b) is a SEM image of Sample B showing a ~1 μm long blister sticking out from the front facet as a result of a significant temperature rise of over 1000°C at the localized spot. Figure 3 (c) and 3 (d) are EBIC images from Sample B and Sample C, respectively. These images show the front facets of both samples where active layers were glowing except at the blister area and clearly indicate that the p-n junction interface surrounding the hot spot or blister was significantly displaced during the COMD process. The formation of DLDs in degraded InGaAs-AlGaAs strained QW lasers with a significant drop in optical power is due to the growth of dislocations. Dark lines or dark areas observed from the active region indicate the presence of localized defects in the active region.



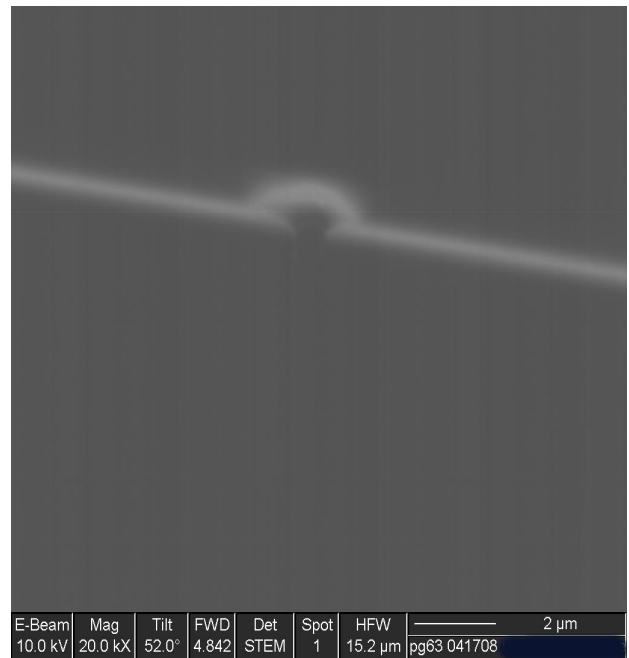
(a)



(b)



(c)



(d)

Figure 3. EBIC images from Sample B (a, c) and Sample C (d). SEM image of Sample B (b).

We also studied broad-area lasers with a 5-10% drop in optical power and no obvious DLDs were observed from these samples. Two types of DLDs have been reported including (100) DLDs and (110) DLDs. (100) DLDs are due to dislocation networks formed by climb motion of pre-existing dislocations, whereas (110) DLDs are due to dislocation networks formed by glide motion of dislocations. Only (110) DLDs were observed from our samples failed by the COMD process. To understand failure mechanisms responsible for catastrophic facet degradation of broad-area lasers, a series of TEM samples were prepared using focused ion beam analysis from laser diode samples failed by COMD. Figure 4 shows a plan view TEM image from Sample A. The EBIC image of this sample is shown in Figure 4 (b), where the location of the TEM sample is indicated as a dotted area. The plan view TEM sample covering an area of $\sim 10\mu\text{m} \times 20\mu\text{m}$ was located $\sim 500\mu\text{m}$ away from the front facet and enclosed three distinctive dark lines. The TEM image clearly shows a high density of dislocations along all three dark lines and the width and separation of three dislocation areas coincided well with those of the dark lines observed from the EBIC image. Detailed defect analysis is necessary to fully understand the very different defect structures observed from the three DLD areas, but it appears that filamentary behavior of the optical beam might be responsible for DLD-3.

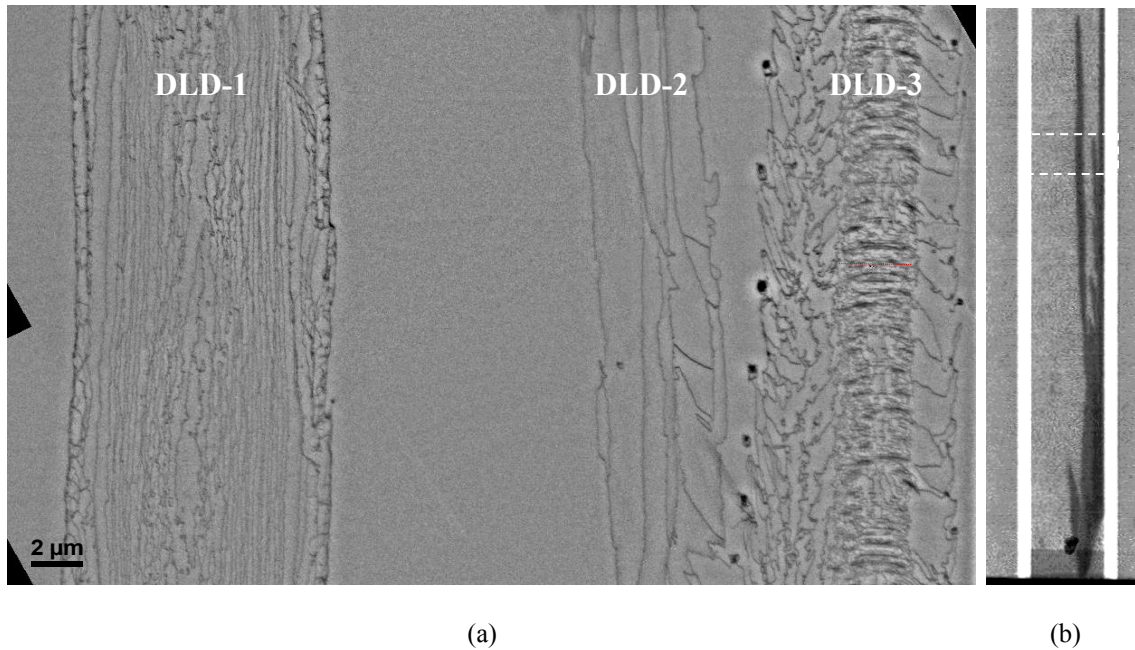


Figure 4. Plan view TEM image from Sample A (a) and EBIC image from Sample A showing the location of TEM sample indicated as a dotted area (b).

Figure 5 shows a SEM image of Sample D, where two TEM samples were prepared. One TEM sample, TEM Sample-D1, was from the DLD area, whereas the other TEM sample, TEM Sample-D2, was not. Both TEM samples were $\sim 20\mu\text{m}$ long and included the front facet. Figure 6 shows cross sectional TEM images from TEM Sample-D1. This sample shows extensive damage introduced to the InGaAs QW and surrounding the SCH layers. TEM Sample-D2 prepared from areas outside of the dark line showed no dislocations.

4. BULK DEGRADATION

Figure 7 shows EBIC images from Sample E and Sample F. Sample E and Sample F were lifetested at 5A and 6A, respectively at the same baseplate temperature of 65°C . Figure 7 shows EBIC images from the whole chip (a) and front facet area (b) of Sample E as well as the EBIC image from Sample F (d). Figure 7 (c) is the EBIC image from the front facet of Sample E near the edge of the waveguide showing a glowing active layer confirming no facet damage introduced to the sample. Two observations that no DLDs were observed near the front facet for Sample E and Sample F and that DLDs of these two samples originated from the inside of the cavity indicate that these samples degraded by bulk failure. Sample E and Sample F showed different amounts of drop in optical output

power. Sample E with a ~60% drop in optical power and Sample F with an ~100% drop. All unpassivated broad-area lasers studied for this investigation failed by COMD, and none of these devices showed bulk failure. In contrast, ~30% of the passivated broad-area lasers tested showed bulk failure, indicating that good passivation increases the threshold for COMD so that it may become larger than the threshold for bulk failure. In addition, all single-mode lasers we previously investigated failed by COMD.

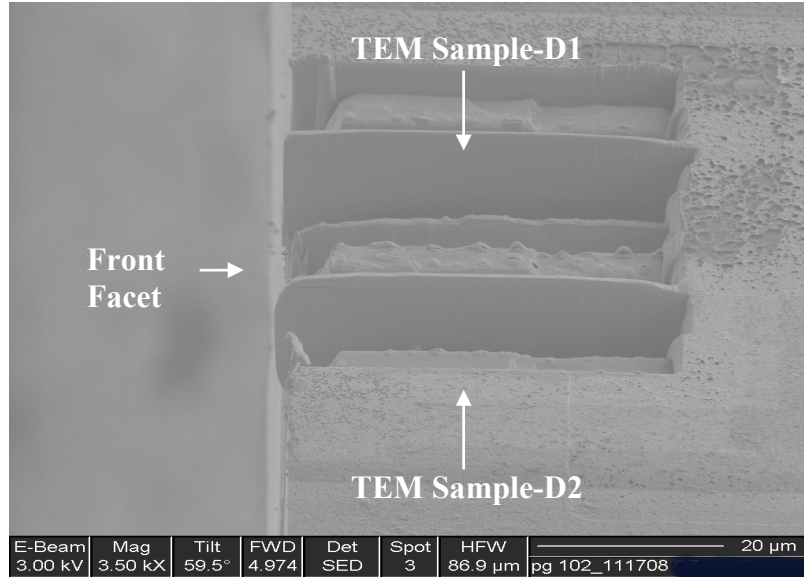


Figure 5. SEM image of Sample D showing the location of two cross sectional TEM samples.

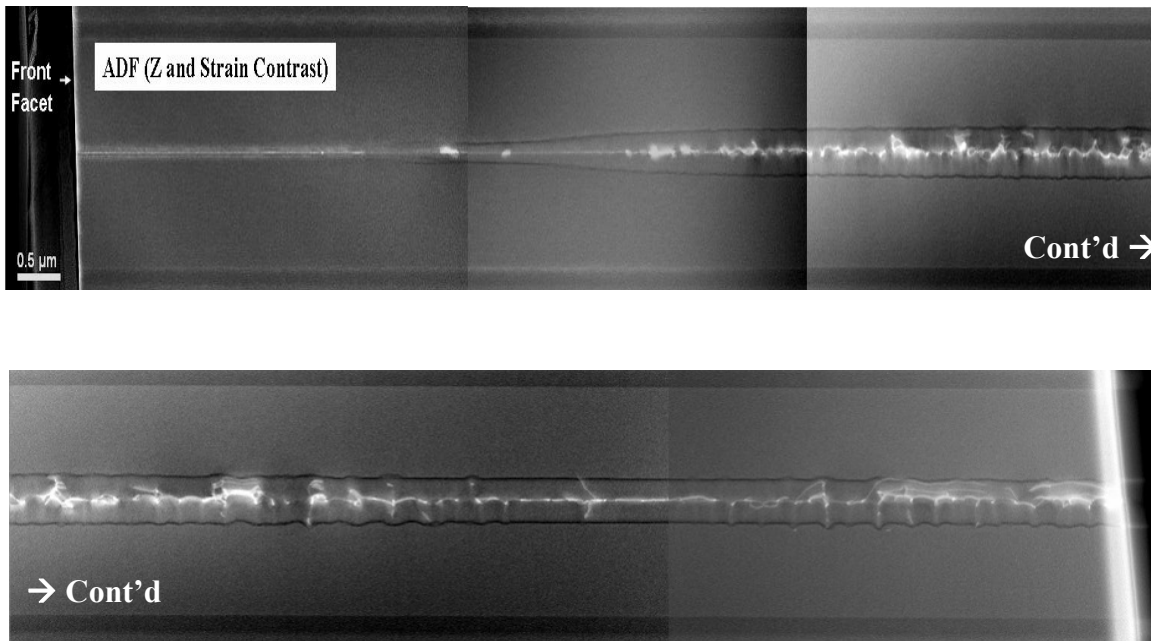
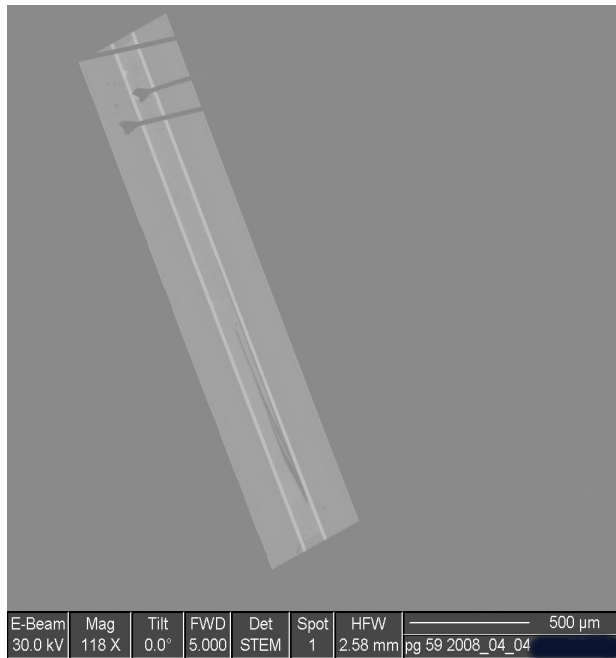
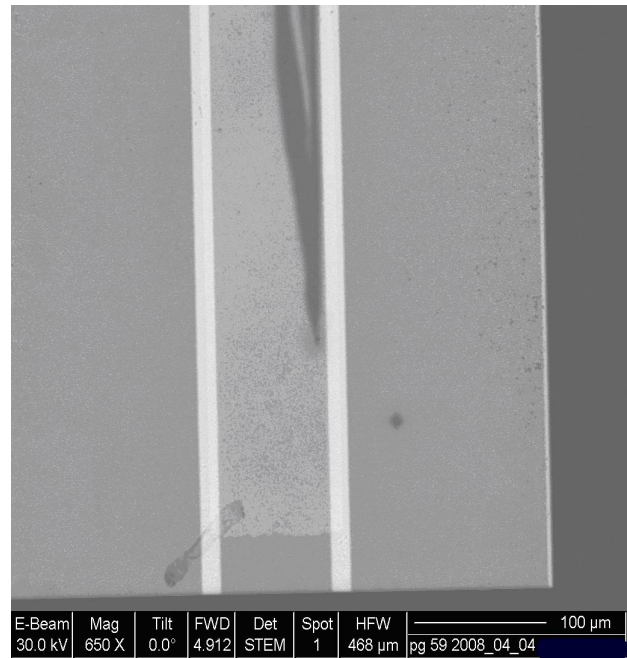


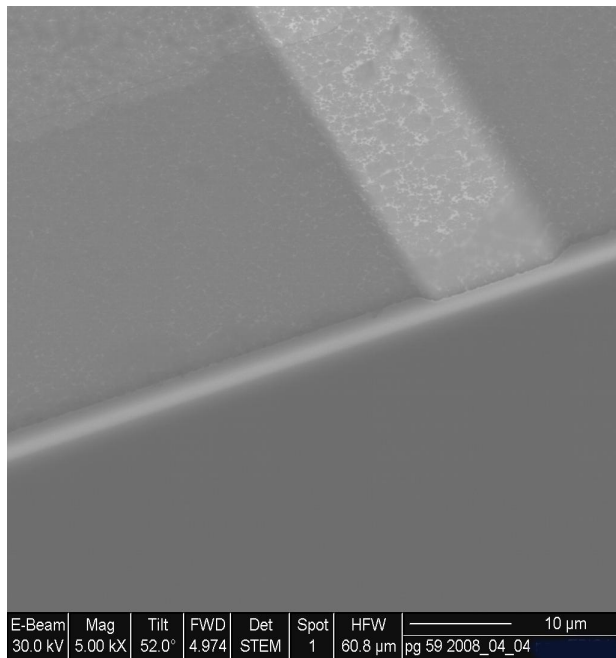
Figure 6. Cross-sectional TEM images of TEM Sample-D1.



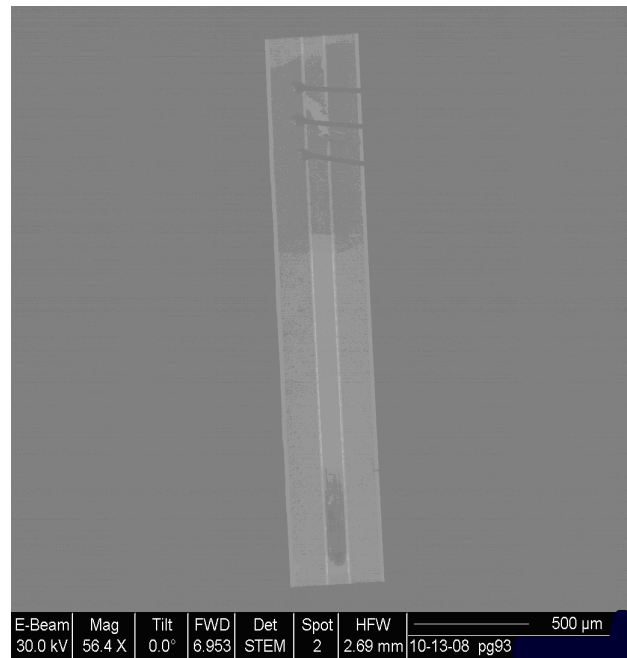
(a)



(b)



(c)



(d)

Figure 7. EBIC images from Sample E (a, b, c) and Sample F (d). EBIC images showing the whole chip (a), area near front facet (b), and front facet (c) of Sample E.

Figure 8 shows EBIC images showing the whole chip (a) and front facet area (b) of Sample G, which showed a ~25% drop in optical power. This sample also degraded by bulk failure. Compared to Sample E and Sample G,

Sample F showed significant bulk damage. It is interesting to note that the three bulk failures (Sample E, Sample F, and Sample G) show a good correlation between amounts of drop in optical power and DLD areas.

Recombination enhanced defect reaction (REDR) was proposed to explain catastrophic sudden degradation in GaAs-based laser diodes, which is possible via two different mechanisms including dislocation climb and dislocation glide [21, 22]. Both mechanisms lead to the nucleation of dislocation dipoles and enable dislocations in motion as devices are in operation. Recombination processes and subsequent localized heating in the vicinity of pre-existing dislocations lead devices to bulk failure.

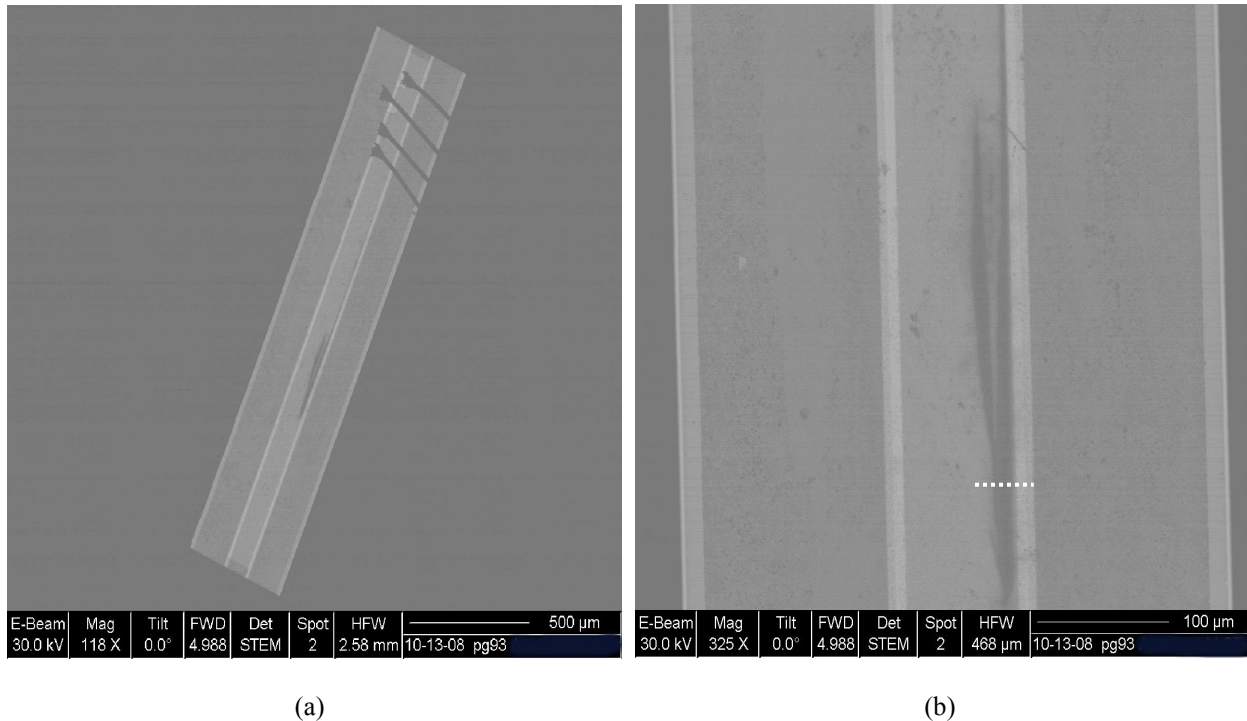
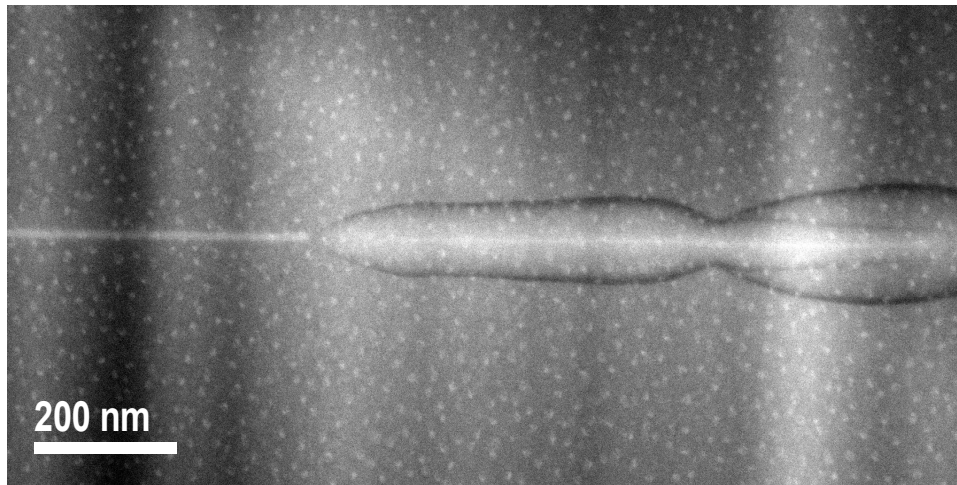


Figure 8. EBIC images showing the whole chip (a) and DLD area (b) of Sample G.

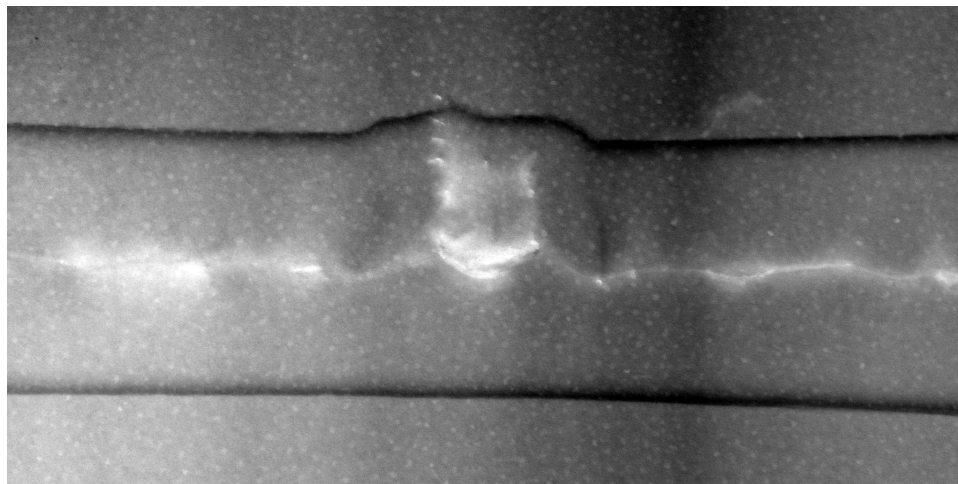
To understand the failure mechanisms responsible for catastrophic bulk degradation of broad-area lasers, a series of TEM samples were prepared from bulk failures using focused ion beam analysis. Figure 9 show TEM images from Sample G. The EBIC image of Sample G is shown in Figure 8 (b), where the location of the TEM sample is shown as a dotted line. The TEM sample was located ~600μm away from the front facet and enclosed the dark line. The TEM image clearly shows a high density of dislocations well confined in the vicinity of the InGaAs quantum well. Detailed TEM analysis is in progress to compare bulk failures with facet failures.

In order to develop a reliability model based on the physics of failure, it is crucial to understand processes leading to device degradation including nucleation and movement of dislocations as devices are aged. Various techniques including laser irradiation [23] and electron beam irradiation [23, 24] were employed to stimulate the glide motion of dislocations in GaAs substrates with and without stress. Several groups also investigated propagation of dislocations in laser diodes where dislocation sources were introduced by damaging the devices with external laser irradiation [25]. The fact that a large discrepancy in dislocation propagation velocities is reported suggests that most of previous studies do not address mechanisms that generate dislocations in the bulk of a laser structure and degradation processes that occur in actual devices under aging and necessitates a better technique to measure the dislocation propagation velocity in devices as they are under aging. The best approach appears to study DLDs in real time developed during aging using a novel non-destructive technique. Our group has recently started developing a time-resolved electroluminescence technique that might enable us to estimate the propagation velocity and

activation energy of dislocation (or dark line defect) motion as the devices are under accelerated aging. Our results will be published elsewhere.



(a)



(b)

Figure 9. Cross sectional TEM images of Sample G (a, b).

4. SUMMARY

We investigated failure modes of catastrophically degraded broad-area InGaAs-AlGaAs strained quantum well single emitters at different stages of degradation using electron beam induced current, focused ion beam, and high-resolution transmission electron microscope techniques. We investigated degraded broad-area lasers failed by COMD and bulk failure. From a series of EBIC images obtained from degraded broad-area lasers exclusively showing (110) dark line defects, we were able to identify the dominant failure modes in both unpassivated and passivated devices. Both cross sectional and plan view TEM analysis shows that a high density of dislocations are well confined in the vicinity of the InGaAs QW and that dark line defects originate from dislocations created during

catastrophic degradation. Detailed defect analysis using HR-TEM is in progress to understand degradation mechanisms responsible for facet failure and bulk failure.

ACKNOWLEDGMENTS

This work was supported under The Aerospace Corporation's Mission Oriented Investigation and Experimentation program, funded by the U.S. Air Force Space and Missile Systems Center under Contract No. FA8802-09-C-0001.

REFERENCES

1. V. Rossin, E. Zucker, M. Peters, M. Everett, and B. Acklin, "High-power high-efficiency 910-980nm broad area laser diodes," *Proc. SPIE* **5336**, pp.196-202, 2004.
2. B. Schmidt, B. Sverdlov, S. Pawlik, N. Lichtenstein, J. Müller, B. Valk, R. Baettig, B. Mayer, and C. Harder, "9xx high-power broad area laser diodes," *Proc. SPIE* **5711**, pp. 201-208, 2005.
3. M. Kanskar, T. Earles, T. Goodnough, E. Stiers, D. Botez, and L. J. Mawst, "High power conversion efficiency Al free diode lasers for pumping high power solid state laser systems," *Proc. SPIE* **5738**, pp. 47-56, 2005.
4. Z. Xu, W. Gao, L. Cheng, A. Nelson, K. Luo, A. Mastrovito, and T. Yang, "High-brightness, high-efficiency 940-980nm InGaAs/AlGaAs/GaAs broad waveguide diode lasers," *Technical Digest of Conference on Lasers and Electro-Optics (CLEO)*, paper CMX4, 2005.
5. V. Gapontsev, I. Berishev, G. Ellis, A. Komissarov, N. Moshegov, O. Raisky, P. Trubenko, V. Ackermann, E. Shcherbakov, J. Steinecke, and A. Ovtchinnikov, "High-efficiency 970 nm multimode pumps," *Proc. SPIE* **5711**, pp. 42-51, 2005.
6. A. H. Paxton and G. C. Dente, "Filament formation in semiconductor laser gain regions," *J. Appl. Phys.* **70**, pp. 2921- 2925, 1991.
7. R. J. Lang, D. Mehuys, D. F. Welch, and L. Goldberg, "Spontaneous filamentation in broad-area diode laser amplifiers," *IEEE J. Quantum Electronics* **30**, pp. 685-694, 1994.
8. A. P. Bogatov, A. E. Drakin, A. A. Stratonnokov, and V. P. Konyaev, "Brightness and filamentation of beam from powerful CW quantum-well In_{0.2}Ga_{0.8}As/GaAs lasers," *Quantum Electronics* **30**, pp. 401-405, 2000.
9. G. C. Dente, "Low confinement factors for suppressed filaments in semiconductor lasers," *IEEE J. Quantum Electronics* **37**, pp. 1650-1653, 2001.
10. J. R. Marciante and G. P. Agrawal, "Spatio-temporal characteristics of filamentation in broad-area semiconductor lasers," *IEEE J. Quantum Electronics* **33**, pp. 1174-1179, 1997.
11. L. Goldberg, M. R. Surette, and D. Mehuys, "Filament formation in a tapered GaAlAs optical amplifier," *Appl. Phys. Lett.* **62**, pp. 2304-2306, 1993.
12. J. R. Marciante and G. P. Agrawal, "Controlling filamentation in broad-area semiconductor lasers and amplifiers," *Appl. Phys. Lett.* **69**, pp. 593-595, 1996.
13. M. Bou Sanayeh, A. Jaeger, W. Schmid, S. Tautz, P. Brick, K. Streubel, and G. Bacher, "Investigation of dark line defects induced by catastrophic optical damage in broad-area AlGaInP laser diodes," *Appl. Phys. Lett.* **89**, 101111, 2006.
14. K. H. Park, J. K. Lee, D. H. Jang, H. S. Cho, C. S. Park, K. E. Pyun, J. Y. Jeong, S. Nahm, and J. Jeong, "Characterization of catastrophic optical damage in Al-free InGaAs/InGaP 0.98 μ m high-power lasers," *Appl. Phys. Lett.* **73**, pp. 2567-2569, 1998.
15. M. Vanzi, G. Salmini, and R. De Palo, "New FIB/TEM evidence for a REDR mechanism in sudden failures of 980nm SL SQW InGaAs/AlGaAs pump laser diodes," *Microel. Reliab.* **40**, pp.1753-1757, 2000.
16. Y. Sin, B. Foran, N. Presser, M. Mason, and S. C. Moss, "Reliability and failure mode investigation of high power multi-mode InGaAs strained quantum well single emitters," *Proc. SPIE* **6456** (High-Power Diode Laser Technology and Applications V), 645605, pp.1-13, 2007.
17. Y. Sin, N. Presser, B. Foran, and S. C. Moss, "Investigation of catastrophic degradation in high power multi-mode InGaAs strained quantum well single emitters", *Proc. SPIE* **6876** (High Power Diode Laser Technology and Applications VI), p.68760R-1 - 68760R-12, 2008.
18. H. J. Leamy, "Charge collection scanning electron microscopy," *J. Appl. Phys.* **53**, pp. R51-R80, 1982.

19. R. G. Waters, D. P. Bour, S. L. Yellen, and N. F. Ruggieri, "Inhibited dark-line defect formation in strained InGaAs/AlGaAs quantum well lasers," *Photonics Technol. Lett.* **2**, pp. 531-533, 1990.
20. S. L. Yellen, A. H. Shepard, R. J. Dalby, J. A. Baumann, H. B. Serreze, T. S. Guido, R. Soltz, K. J. Bystrom, C. M. Harding, and R. G. Waters, "Reliability of GaAs-based semiconductor diode lasers: 0.6-1.1 μm ," *J. Quantum. Electron.* **29**, pp. 2058-2067, 1993.
21. L. C. Kimerling, "Recombination enhanced defect reactions," *Solid State Electron* **38**, pp. 1391-1401, 1978.
22. A. Bonfiglio, M. Vanzi, M. B. Casu, F. Magistrali, M. Maini, and G. Salmini, "Interpretation of sudden failures in pump laser diodes," Proceedings from the 23rd International Symposium for Testing and Failure Analysis, Santa Clara, California, pp. 189-194, October 1997.
23. P. G. Eliseev, "Optical strength of semiconductor laser materials," *Prog. Quantum. Electron.* **20**, pp. 1-82, 1996.
24. K. Maeda, M. Sato, A. Kubo, and S. Takeuchi, "Quantitative measurements of recombination enhanced dislocation glide in gallium arsenide," *J. Appl. Phys.* **54**, pp. 161-168, 1983.
25. C. H. Henry, P. M. Petroff, R. A. Logan, and F. R. Merritt, "Catastrophic damage of $\text{Al}_x\text{Ga}_{1-x}\text{As}$ double-heterostructure laser material," *J. Appl. Phys.* **50**, pp. 3721-3732, 1979.